


 Cite this: *Chem. Commun.*, 2026, 62, 5980

 Received 8th January 2026,
Accepted 11th February 2026

DOI: 10.1039/d6cc00146g

rsc.li/chemcomm

Bis(*N*-heterocyclic carbene)-borylene-mediated heteroallene activation

 An-Ping Koh,^{†a} Gaël Vernezoul,^{†a} Jun Fan,^{†a} Zheng-Feng Zhang,^b
Ming-Der Su^{†bc} and Cheuk-Wai So^{†*a}

This study describes a bis(*N*-heterocyclic carbene)-borylene that activates heteroallenes. The borylene undergoes a bora-Staudinger reaction with azide to afford an NHC-iminoborane, and also catalyzes the cyclotrimerization of isocyanates to give isocyanurates. In the presence of excess pinacolborane, it catalyzes the chemoselective hydroboration of isocyanates to form *N*-boryl formamides.

Low-oxidation-state boron derivatives with pronounced electrophilic and/or nucleophilic character effectively mimic transition metals in the activation of enthalpically strong bonds and small molecules.¹ In this context, borylenes R-B: (R = substituent), which contain a lone pair of electrons and two empty orbitals, have captured significant attention.² Free mono-coordinate borylenes, such as H₂N-B:, F-B: and Ph-B: are transient and observed spectroscopically in inert gas matrices at very low temperatures.³ The coordination of a Lewis base to this Lewis-ambiphilic B(I) center can significantly enhance borylene stability. In 2011, Bertrand and co-workers demonstrated that the parent borylene H-B: can be stabilized by two cyclic (alkyl)(amino)carbenes (CAACs), affording a borylene complex featuring a nucleophilic B(I) center.⁴ Since then, numerous three-coordinate borylenes supported by various Lewis bases have been isolated, many of which exhibit remarkable nucleophilic and reducing ability.^{5–11} By decreasing the number of supporting Lewis bases, Bertrand, Stephan, and co-workers subsequently showed that a stable two-coordinate cAAC-aminoborylene complex displays transition-metal-like activation of dihydrogen and carbon monoxide.¹² Braunschweig and co-workers further discovered that transient two-coordinate cAAC-arylborylenes are capable of activating and

functionalizing dinitrogen.¹³ Driess *et al.* showed that a transient bis(two-coordinate NHC-borylene) mediated the deoxygenation of a -C-O-C- skeleton.¹⁴ More recently, alternative strategies for the *in situ* generation of two-coordinate base-stabilized borylenes through ligand dissociation of a bis-base-stabilized three-coordinate borylene have emerged.^{15,16} Cummins, Gilliard, and co-workers demonstrated that the thermal extrusion of dinitrogen from a diazoborane produces a reactive *N*-heterocyclic carbene (NHC)-mesitylborylene that can be transferred to suitable substrates.¹⁷ They also showed that transient cAAC-haloborylenes can be released from boranorbornadienes.¹⁸ In addition, Braunschweig and co-workers reported the *in situ* formation of two-coordinate cAAC-arylborylene, cAAC-borylborylene and cAAC-cyclohexylborylene *via* the dissociation of CO and phosphine ligands from their respective three-coordinate borylene complexes.^{19–21}

However, catalytic organic transformations mediated by low-oxidation-state boron compounds remain surprisingly underexplored. Two examples have been reported. First, Wang, Mo, and co-workers illustrated that a bis(silylene)-amidoborylene complex can serve as a precatalyst, reacting with CO₂ to generate an oxo-bridged boryl-anion-silylium-cation species that catalyzes the *N*-formylation of amines using CO₂ and HBpin.²² Second, we showed that an *N*-phosphinoamidinato NHC-diborene complex catalyzes the hydroboration of CO₂ with HBpin.²³

Recently, we reported the bis(NHC)-arylborylene complex [(IME)₂BMes] (**1**, IMe = :C{N(Me)C(Me)}₂, Mes = mesityl) that exhibits strong nucleophilic character and is capable of capturing and stoichiometrically functionalizing carbon dioxide.²⁴ Building on this reactivity, we hypothesized that compound **1** should also be competent for the functionalization and/or catalytic transformation of other heteroallenes, namely, azide and isocyanate.

To begin our study, diisopropylphenyl azide (DippN₃) was examined. Compound **1** underwent the bora-Staudinger reaction with DippN₃ in toluene at room temperature for 4 h to afford the NHC-iminoborane [(IME)MesB=NDipp] (**2**, yield: 76%,

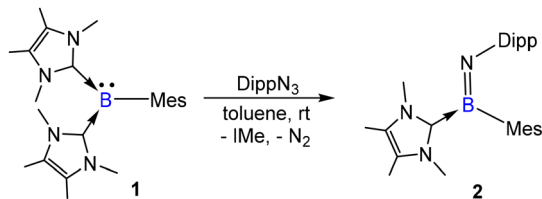
^a School of Chemistry, Chemical Engineering and Biotechnology, Nanyang Technological University, Singapore 637371, Singapore. E-mail: CWSO@ntu.edu.sg

^b Department of Applied Chemistry, National Chiayi University, Chiayi 60004, Taiwan. E-mail: midesu@mail.ncyu.edu.tw

^c Department of Medicinal and Applied Chemistry, Kaohsiung Medical University, Kaohsiung 80708, Taiwan

† Equal contribution.



Scheme 1 Synthesis of **2**.

Scheme 1), along with the displacement of N_2 and IMe. Compound **2** was isolated as a yellow crystalline solid from the concentrated reaction mixture. Such Staudinger-type reactivity of a three-coordinate bis(Lewis base)-stabilized borylene complex to form a Lewis base-stabilized iminoborane through ligand dissociation has not been reported before. Moreover, the dissociation of an NHC ligand from a borylene center is rare. In addition to our method, carbene-iminoboranes are commonly synthesized by 1,2-elimination of suitable boranamine precursors.²⁵ The $^{11}B\{^1H\}$ NMR signal of compound **2** (22.0 ppm) is in the range of reported ^{11}B NMR signals of three-coordinate boron centers in carbene-iminoborane complexes (12.4–24 ppm).²⁶ The molecular structure obtained *via* X-ray crystallography shows that the B–N bond (1.355(5) Å, Fig. 1) is typical of a double bond.

The reactivity of compound **1** toward isocyanates was further examined. Cyclotrimerization of the isocyanates was observed using both stoichiometric and catalytic amounts of **1**. These results indicate that compound **1** exhibits catalytic activity. In this context, 3 mol% of compound **1** was used to catalyze the cyclotrimerization of the aryl isocyanate $ArNCO$ ($Ar = 4-CH_3C_6H_4$ (**3a**), Table 1), as well as its derivatives with electron-donating ($Ar = 4-MeOC_6H_4$ (**3b**)) and electron-withdrawing substituents ($Ar = 4-FC_6H_4$ (**3c**), $4-NCC_6H_4$ (**3d**)) in C_6D_6 at room temperature for 5 min, which afforded aryl isocyanurates **4a–4d** in moderate-to-high isolated yields (64–94%). As expected, a longer reaction time was required for the catalytic cyclotrimerization of sterically hindered mesityl isocyanate (**3e**), diisopropylphenyl isocyanate (**3f**), and 1-naphthyl isocyanate (**3g**) to afford the corresponding products **4e–4g** in good isolated yields (57–95%, TOF: 0.26–66 h^{-1}). Second, the cyclotrimerization of non-aromatic isocyanates, namely, benzylisocyanate (**4h**), 4-methoxybenzylisocyanate (**4i**), and 2,2-diphenylethyl isocyanate (**4j**), was also achieved in moderate-to-high isolated yields (57–96%, TOF: 0.45–370 h^{-1}).

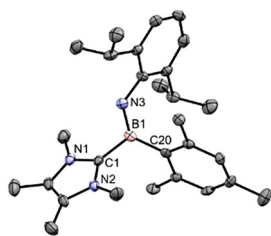
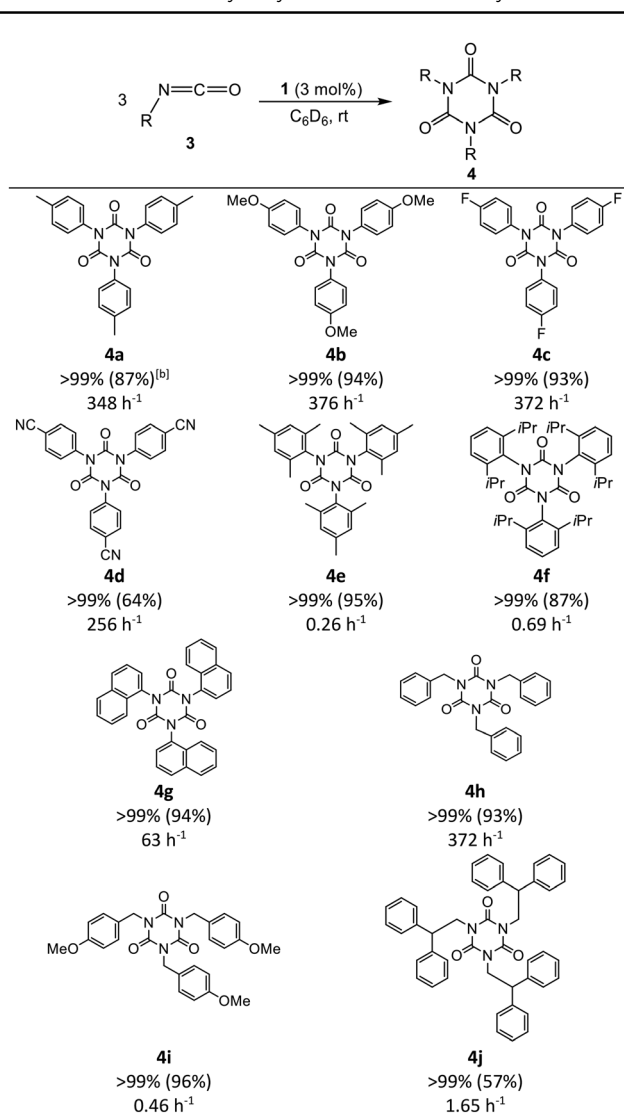


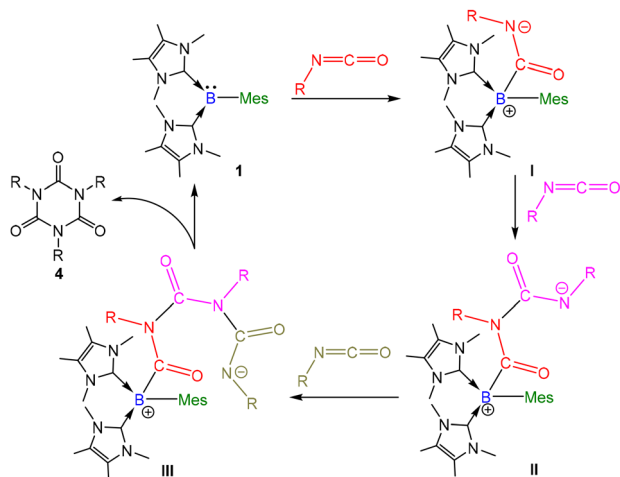
Fig. 1 Molecular structure of **2** obtained by X-ray crystallography. Thermal ellipsoids are shown at 50% probability. All hydrogen atoms have been removed for clarity. Selected bond lengths (Å) and angles (deg): B1–N3 1.355(5), B1–C1 1.616(5), C1–N1 1.362(4), C1–N2 1.346(4), C1–B1–N3 114.1(3), C20–B1–N3 129.8(3), C1–B1–C20 116.0(3).

Table 1 1-mediated catalytic cyclotrimerization of isocyanates^a

^a Reaction conditions: isocyanate substrates (0.30 mmol), C_6D_6 (0.40 mL), catalyst **1** (3 mol%). ^b NMR yields were determined *via* 1H NMR spectroscopy based on the resonances of the products with reference to the internal standards cyclohexane or 1,3,5-trimethoxybenzene. Isolated yields are reported in parentheses. All the catalytic trials were repeated in triplicate.

Third, after the full conversion of *p*-tolyl isocyanate **4a**, the reaction mixture was analyzed using $^{11}B\{^1H\}$ NMR spectroscopy. A major signal at -6.9 ppm was observed in the spectrum, indicating the regeneration of compound **1** (Fig. S4). In the catalysis, the borylene center in compound **1** attacks an isocyanate to form $[(IME)_2(Mes)BC(NAr)(=O)]$ (**I**, Scheme 2). The negatively charged nitrogen center subsequently attacks a second isocyanate molecule to form $[(IME)_2(Mes)B\{C(=O)(NAr)\}_2]$ (**II**). This reacts with a third isocyanate molecule to form $[(IME)_2(Mes)B\{C(=O)(NAr)\}_3]$ (**III**), the terminal two-coordinated nitrogen atom of which undergoes an intramolecular nucleophilic attack on the boron-bonded carbonyl center to afford the six-membered isocyanurate **4** and regenerate compound **1**. Similar mechanisms have been found in the catalytic cyclotrimerization





Scheme 2 Proposed mechanism of the catalytic cyclotrimerization of isocyanates.

of isocyanates mediated by an NHC,²⁷ *N*-heterocyclic olefin,²⁸ proazaphosphatane,²⁹ 2-phosphaethynolate anion³⁰ and NHC-silyliumylidene cation.³¹

Due to the ability of compound **1** to demonstrate catalytic cyclotrimerization, we attempted to explore the catalytic hydroboration of isocyanates with HBpin. 1 mol% of compound **1** could not catalyze the hydroboration of *p*-tolyl isocyanate with 1 equivalent of HBpin, as catalytic cyclotrimerization occurred (entry 1, Table 2). Upon increasing the amount of HBpin to 5 equivalents, the catalytic hydroboration of *p*-tolyl isocyanate proceeded smoothly at room temperature, giving the corresponding *N*-borylated formamide with 19% conversion (entry 2, Table 2). This indicates that the presence of excess HBpin

Table 2 Catalytic optimization of the hydroboration of *p*-tolyl isocyanate with HBpin

Entry	Y (mol%)	<i>n</i> (eq.)	<i>T</i> (°C)	Time (h)	Yield (%)	
					5a ^a	6a ^b
1	1	1	25	8	<1	<1
2	1	5	25	5	19	6
3	3	5	25	6	93	7
4 ^c	5	5	25	6	96	6

Reaction conditions: required amount of isocyanate substrates (0.30 mmol), required amount of **1** (1, 3 or 5 mol%), required amount of HBpin (0.30 or 1.50 mmol) and C₆D₆ (0.40 mL) in a J-Young NMR tube. ^a NMR yield of *N*-borylated formamide **5a** was determined via ¹H NMR spectroscopy based on isocyanate consumption and the appearance of the NC(=O)H signal. ^b NMR yield of *N*,*O*-bis(boryl)-hemiaminal **6a** was determined via ¹H NMR spectroscopy based on *N*-borylated formamide consumption and the appearance of the NCH₂OBpin signal. The catalytic trials were repeated in triplicate. ^c Optimized conditions.

prevents intermediate **I** (Scheme 2) from reacting with the second molecule of isocyanate. Optimizing the catalyst loading of compound **1** to 5 mol% further improved the reaction outcome, increasing the conversion of the *N*-borylated formamide to 96%.

With the optimized parameters in hand, the scope and selectivity were then investigated (Table 3). The hydroboration of aromatic isocyanates containing electron-donating and electron-withdrawing substituents converted them to the respective *N*-borylated formamides (**5a–5h**, isolated yields of **7a–7h**: 62–92%). Non-aromatic isocyanates were also hydroborated to their respective *N*-borylated formamides (**5i–5j**, isolated yields of **7i–7j**: 88–96%). Interestingly, although the hydroboration of aromatic isocyanates afforded small quantities of the *N*,*O*-bis(boryl) hemiaminal species, the hydroboration of non-aromatic isocyanates yielded the *N*-borylated formamide exclusively.

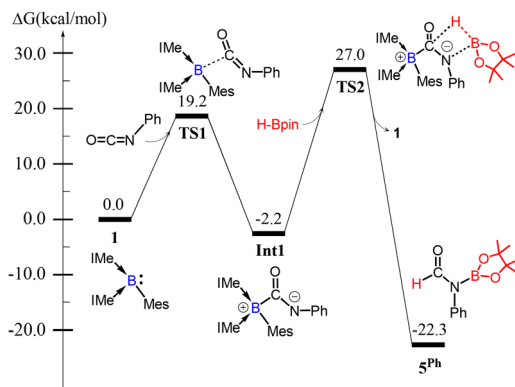
The catalytic mechanism for the **1**-catalyzed hydroboration of phenyl isocyanate was studied using DFT calculations (Scheme 3). The borylene center in **1** first attacks the carbon atom of phenyl isocyanate through **TS1** ($\Delta G^\ddagger = 19.2$ kcal mol⁻¹) to form [(IME)₂(Mes)BC(NPh)(=O)] (**Int 1**, $\Delta G = -2.2$ kcal mol⁻¹).

Table 3 Scope of isocyanate substrates^a

R	Yield (%)	Time (h)
	>96% (62%) ^b	9.6 h ⁻¹
	>96% (70%)	12.8 h ⁻¹
	>98% (69%)	9.8 h ⁻¹
	>94% (80%)	9.4 h ⁻¹
	>98% (90%)	9.8 h ⁻¹
	>85% (81%)	5.67 h ⁻¹
	>96% (92%),	12.8 h ⁻¹
	>99% (86%)	39.6 h ⁻¹
	>99% (96%)	15.2 h ⁻¹
	>99% (88%)	3.96 h ⁻¹

^a Reaction conditions: Isocyanate substrate (0.30 mmol), C₆D₆ (0.40 mL), catalyst **1** (5 mol%). ^b NMR yields of **5** were determined via ¹H NMR spectroscopy based on isocyanate consumption and the appearance of the NC(=O)H signal. Isolated yields of **7** are reported in parentheses. All the catalytic trials were repeated in triplicate.





Scheme 3 Catalytic mechanism for the **1**-mediated hydroboration of isocyanates.

The negatively charged nitrogen center subsequently attacks the boron center of HBpin, while the hydrogen atom of HBpin attacks the carbonyl group *via* a 4-membered-ring transition state (TS2, $\Delta G^\ddagger = 27.0 \text{ kcal mol}^{-1}$), which leads to the formation of product **5^{Ph}** and regeneration of catalyst **1** ($\Delta G = -22.3 \text{ kcal mol}^{-1}$).

In conclusion, bis(*N*-heterocyclic carbene)-mesitylborylene **1** mediated the bora-Staudinger reaction with azide to form the NHC-iminoborane, as well as the catalytic cyclotrimerization and chemoselective hydroboration of isocyanates to form isocyanurates and *N*-borylated formamides, respectively.

A.-P. Koh and G. Vernezoul designed and conducted the catalytic studies. J. Fan carried out the azide activation. Z.-F. Zhang and M.-D. Su designed and performed the DFT calculations. All authors have given approval to the final version of the manuscript.

Conflicts of interest

There are no conflicts to declare.

Data availability

The supporting data has been provided as part of the supplementary information (SI). Supplementary information: experimental details, NMR spectra and DFT calculations. See DOI: <https://doi.org/10.1039/d6cc00146g>.

CCDC 2270478 (**2**), 2257721 (**4a**), 2257722 (**4b**), 2257723 (**4c**), 2257724 (**4d**), 2257725 (**4e**), 2257726 (**4h**), 2517514 (**4j**) contain the supplementary crystallographic data for this paper.^{32a-h}

Acknowledgements

This work is supported by the Ministry of Education Singapore, AcRF Tier 1 (RG8/25) and A*STAR MTC Individual Research Grants (M21K2c0117). M.-D. Su acknowledges the National Center for High-Performance Computing of Taiwan for generous amounts of computing time, and the Ministry of Science and Technology of Taiwan for the financial support

Notes and references

- M.-A. Légaré, C. Pranckevicius and H. Braunschweig, *Chem. Rev.*, 2019, **119**, 8231–8261.
- M. Soleilhavoup and G. Bertrand, *Angew. Chem., Int. Ed.*, 2017, **56**, 10282–10292 and reference therein.
- (a) P. L. Timms, *J. Am. Chem. Soc.*, 1967, **89**, 1629–1632; (b) C. A. Thompson, L. Andrews, J. M. L. Martin and J. El-Yazal, *J. Phys. Chem.*, 1995, **99**, 13839–13849; (c) K. Edel, M. Krieg, D. Grote and H. F. Bettinger, *J. Am. Chem. Soc.*, 2017, **139**, 15151–15159.
- R. Kinjo, B. Donnadiou, M. A. Celik, G. Frenking and G. Bertrand, *Science*, 2011, **333**, 610–613.
- H. Braunschweig, R. D. Dewhurst, F. Hupp, M. Nutz, K. Radacki, C. W. Tate, A. Vargas and Q. Ye, *Nature*, 2015, **522**, 327–330.
- L. Kong, Y. Li, R. Ganguly, D. Vidovic and R. Kinjo, *Angew. Chem., Int. Ed.*, 2014, **53**, 9280–9283.
- A. Gärtner, L. Meier, M. Arrowsmith, M. Dietz, I. Krummenacher, R. Bertermann, F. Fantuzzi and H. Braunschweig, *J. Am. Chem. Soc.*, 2022, **144**, 21363–21370.
- C. Pranckevicius, C. Herok, F. Fantuzzi, B. Engels and H. Braunschweig, *Angew. Chem., Int. Ed.*, 2019, **58**, 12893–12897.
- D. A. Ruiz, M. Melaimi and G. Bertrand, *Chem. Commun.*, 2014, **50**, 7837–7839.
- M. Arrowsmith, S. Endres, M. Heinz, V. Nestler, M. C. Holthausen and H. Braunschweig, *Chem. – Eur. J.*, 2021, **27**, 17660–17668.
- (a) H. Wang, L. Wu, Z. Lin and Z. Xie, *J. Am. Chem. Soc.*, 2017, **139**, 13680–13683; (b) H. Wang, L. Wu, Z. Lin and Z. Xie, *Angew. Chem., Int. Ed.*, 2018, **57**, 8708–8713; (c) H. Wang, J. Zhang, H. K. Lee and Z. Xie, *J. Am. Chem. Soc.*, 2018, **140**, 3888–3891.
- F. Dahcheh, D. Martin, D. W. Stephan and G. Bertrand, *Angew. Chem., Int. Ed.*, 2014, **53**, 13159–13163.
- (a) M. A. Légaré, G. Bélanger-Chabot, R. D. Dewhurst, E. Welz, I. Krummenacher, B. Engels and H. Braunschweig, *Science*, 2018, **359**, 896–900; (b) M.-A. Légaré, M. Rang, G. Bélanger-Chabot, J. I. Schweizer, I. Krummenacher, R. Bertermann, M. Arrowsmith, M. C. Holthausen and H. Braunschweig, *Science*, 2019, **363**, 1329–1332; (c) M.-A. Légaré, G. Bélanger-Chabot, M. Rang, R. D. Dewhurst, I. Krummenacher, R. Bertermann and H. Braunschweig, *Nat. Chem.*, 2020, **12**, 1076–1080; (d) A. Gärtner, U. S. Karaca, M. Rang, M. Heinz, P. D. Engel, I. Krummenacher, M. Arrowsmith, A. Hermann, A. Matler, A. Rempel, R. Witte, H. Braunschweig, M. C. Holthausen and M.-A. Légaré, *J. Am. Chem. Soc.*, 2023, **145**, 8231–8241; (e) M. Rang, M. Heinz, A. Halkić, M. Weber, R. D. Dewhurst, A. Rempel, M. Härterich, M. C. Holthausen and H. Braunschweig, *J. Am. Chem. Soc.*, 2024, **146**, 11048–11053.
- J. Fan, S. Pan, S. Yao, C. Ding, G. Frenking and M. Driess, *J. Am. Chem. Soc.*, 2025, **147**, 6925–6933.
- M. Arrowsmith, D. Auerhammer, R. Bertermann, H. Braunschweig, G. Bringmann, M. A. Celik, R. D. Dewhurst, M. Finze, M. Grüne, M. Hailmann, T. Hertle and I. Krummenacher, *Angew. Chem., Int. Ed.*, 2016, **55**, 14464–14468.
- H. Braunschweig, I. Krummenacher, M.-A. Légaré, A. Matler, K. Radacki and Q. Ye, *J. Am. Chem. Soc.*, 2017, **139**, 1802–1805.
- C. Zhang, C. C. Cummins and R. J. Gilliard, *Science*, 2024, **385**, 327–331.
- C. Zhang, R. J. Gilliard and C. C. Cummins, *Chem. Sci.*, 2024, **15**, 17873–17880.
- C. Pranckevicius, M. Weber, I. Krummenacher, A. K. Phukan and H. Braunschweig, *Chem. Sci.*, 2020, **11**, 11055–11059.
- Y. Konrad, A. Jayaraman, I. Krummenacher and H. Braunschweig, *Angew. Chem., Int. Ed.*, 2025, **64**, e202423669.
- M. Michel, L. Endres, F. Fantuzzi, I. Krummenacher and H. Braunschweig, *Chem. Sci.*, 2025, **16**, 5632–5639.
- X. Chen, Y. Yang, H. Wang and Z. Mo, *J. Am. Chem. Soc.*, 2023, **145**, 7011–7020.
- J. Fan, J.-Q. Mah, M.-C. Yang, M.-D. Su and C.-W. So, *J. Am. Chem. Soc.*, 2021, **143**, 4993–5002.
- J. Fan, A.-P. Koh, C.-S. Wu, M.-D. Su and C.-W. So, *Nat. Commun.*, 2024, **15**, 3052.
- Y. Fan, J. Cui and L. Kong, *Eur. J. Org. Chem.*, 2022, e202201086.
- P. Cui, R. Guo, L. Kong and C. Cui, *Inorg. Chem.*, 2020, **59**, 5261–5265.
- H. A. Duong, M. J. Cross and J. Louie, *Org. Lett.*, 2004, **6**, 4679–4681.



- 28 C. Li, W. Zhao, J. He and Y. Zhang, *Chem. Commun.*, 2019, **55**, 12563–12566.
- 29 S. M. Raders and J. G. Verkade, *J. Org. Chem.*, 2010, **75**, 5308–5311.
- 30 D. Heift, Z. Benkó, H. Grützmacher, A. R. Jupp and J. M. Goicoechea, *Chem. Sci.*, 2015, **6**, 4017–4024.
- 31 Y.-C. Teo, D. Loh, B.-X. Leong, Z.-F. Zhang, M.-D. Su and C.-W. So, *Inorg. Chem.*, 2023, **62**, 16867–16873.
- 32 (a) CCDC 2270478: Experimental Crystal Structure Determination, 2026, DOI: [10.5517/ccdc.csd.cc2g6m7k](https://doi.org/10.5517/ccdc.csd.cc2g6m7k); (b) CCDC 2257721: Experimental Crystal Structure Determination, 2026, DOI: [10.5517/ccdc.csd.cc2fsbq9](https://doi.org/10.5517/ccdc.csd.cc2fsbq9); (c) CCDC 2257722: Experimental Crystal Structure Determination, 2026, DOI: [10.5517/ccdc.csd.cc2fsbrb](https://doi.org/10.5517/ccdc.csd.cc2fsbrb); (d) CCDC 2257723: Experimental Crystal Structure Determination, 2026, DOI: [10.5517/ccdc.csd.cc2fsbsc](https://doi.org/10.5517/ccdc.csd.cc2fsbsc); (e) CCDC 2257724: Experimental Crystal Structure Determination, 2026, DOI: [10.5517/ccdc.csd.cc2fsbtd](https://doi.org/10.5517/ccdc.csd.cc2fsbtd); (f) CCDC 2257725: Experimental Crystal Structure Determination, 2026, DOI: [10.5517/ccdc.csd.cc2fsbvf](https://doi.org/10.5517/ccdc.csd.cc2fsbvf); (g) CCDC 2257726: Experimental Crystal Structure Determination, 2026, DOI: [10.5517/ccdc.csd.cc2fsbwg](https://doi.org/10.5517/ccdc.csd.cc2fsbwg); (h) CCDC 2517514: Experimental Crystal Structure Determination, 2026, DOI: [10.5517/ccdc.csd.cc2qhp42](https://doi.org/10.5517/ccdc.csd.cc2qhp42).

